Dynamics of alkali-metal atom photodesorption from polymer thin films

J. Brewer,[1] V. G. Bordo,[2] M. J. Kasprowicz,[3] and H.-G. Rubahn[1]
[1]*Fysisk Institut, Syddansk Universitet, DK-5230 Odense M, Denmark*
[2]*Natural Sciences Center, A.M. Prokhorov General Physics Institute, Russian Academy of Sciences, 119991 Moscow, Russia*
[3]*Marian Smoluchowski Institute of Physics, Jagiellonian University, Reymonta 4, 30-059, Poland*
(Received 23 December 2003; published 7 June 2004)

Kinetic energy distributions of alkali-metal atoms (sodium and rubidium) desorbed from polydimethylsiloxane coated glasses via visible (532 nm) and near-infrared (1064 nm) laser irradiation are determined. In each case the time-of-flight spectra show a single desorption peak. In the case of sodium the mean kinetic energy of the desorbing atoms depends on the photon energy and linearly on the laser fluence. Evanescent-wave desorption measurements show that the origin of the desorbed atoms is within the bulk of the thin organic film. The results are discussed in terms of electronic excitation and resonant heating, providing values of barrier heights for desorption from PDMS. The observed small barrier heights explain the weak light intensity necessary for light-induced atomic desorption from such systems.

DOI: 10.1103/PhysRevA.69.062902 PACS number(s): 79.20.La, 68.43.Tj, 68.47.Mn

I. INTRODUCTION

The light-induced desorption of alkali atoms adsorbed on or in dielectric substrates as either isolated atoms, aggregates, or films is of large interest from both applied and fundamental points of view since it resembles a rather unusual form of laser ablation or desorption. Among other peculiarities we mention surface-plasmon-assisted laser desorption [1], the origin of alkali-metal atoms in extraterrestrial atmospheres [2,3], or the light-induced atomic desorption (LIAD) process [4–7].

Astrophysical interest in photon-stimulated alkali-metal desorption stems from the observation of significant amounts of neutral alkali-metal atoms (sodium and potassium) in the atmospheres of the Moon, Mercury, or the Jovian satellite Europa. Since these atmospheres are nonpermanent, it has been suggested that the alkali-metal atoms are resupplied via photon-stimulated desorption processes. Experiments on amorphous silica as well as lunar basalt samples, decorated with submonolayer coverages of alkali metals, support this suggestion [2,3]. UV photons with energies higher than 4 eV (310 nm) result in neutral atom desorption with mean kinetic energies of 100 meV. This is believed to be due to a transfer of hot electrons from the substrate to the unoccupied states of the ionic bound alkali metals with subsequent neutralization and repulsion [8]. The same desorption induced by electronic transitions (DIET) mechanism is probably responsible for UV-laser-induced desorption of isolated potassium atoms from epitaxial layers of $Cr_2O_3(0001)$, where mean kinetic energies of 650 meV were found at very low coverage, decreasing to 260 meV at saturation coverage [9]. These kinetic energies were found to be independent of photon energies (3.5 eV, 5 eV, and 6.4 eV— i.e., 351 nm, 248 nm, and 193 nm) and the velocity distributions could not be fitted by Boltzmann distributions. Upon alkali-metal aggregate formation decreased translational energies of 160 meV were found and interpreted via quenching of the electronically excited states by the metal electrons.

The investigation of the simplest form of desorption of alkali-metal atoms from rough alkali-metal films on dielectrics has a rather long history. Beginning with investigations of laser-induced desorption of sodium atoms from Na films adsorbed on multicrystalline sapphire and quartz surfaces [10], systematic studies have been performed for rough alkali-metal films adsorbed on lithium fluoride [11] and mica surfaces [12]. In fact, under most circumstances Na forms clusters upon adsorption on dielectrics. The clusters exhibit pronounced multipole resonances. Optical excitation on these resonances results in a collective electronic excitation (surface plasmon excitation), which is accompanied by a strong electromagnetic field enhancement on the surface of the clusters. In turn, this leads to nonthermal desorption of atoms from the alkali-metal surface.

Systematic measurements have revealed subthermal distributions of the desorbing atoms with kinetic energies of 20 meV [1]. The full velocity distributions could be reproduced by a quantum-mechanical multiphonon scattering model. In the framework of this model it has been argued that the shallow well (a few hundred meV) of the binding potential skews the energy distribution of desorbed particles since only the low-energy part of the distribution of impinging particles will stick and only the trapped particles will be observed in laser-induced desorption (microscopic reversibility). In fact, the laser excitation will eventually result in a distribution of low-kinetic-energy neutral atoms in the vicinity of the surface, which will exchange energy with the surface via multiphonon excitation-deexcitation processes provided that (i) the particles have large mass, (ii) their masses equal the mass of the surface atoms, and (iii) the surface temperature is high compared to the Debye temperature. These conditions are well fulfilled for alkali-metal desorption from rough alkali-metal films on dielectrics.

Alternatively to the above desorption model it has been suggested that the interaction of light with rough alkali-metal films and the concomitant excitation of surface plasmons could also lead directly to the creation of antibonding pairs at defect sites and thus desorption. This mechanism would explain several experimentally observed characteristics of laser-induced alkali-metal desorption from alkali-metal layers on dielectrics too [11], but it cannot explain the observed

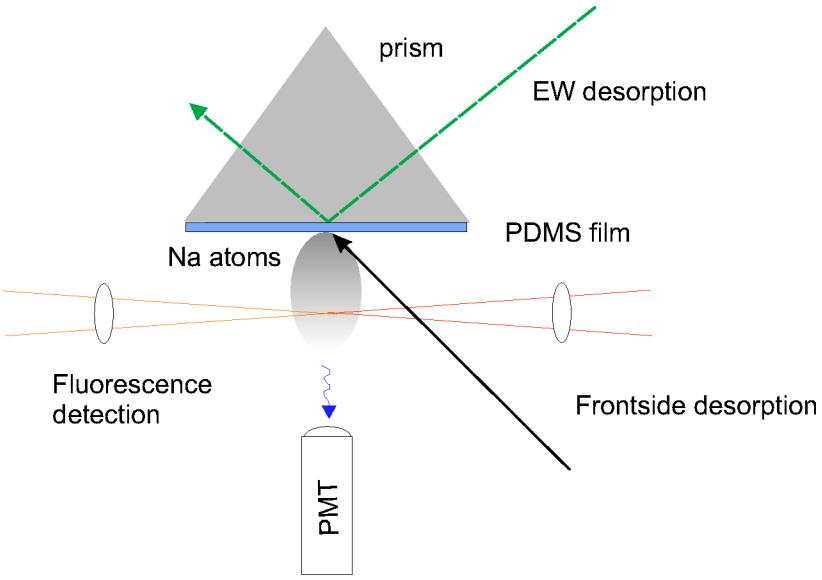

FIG. 1. Experimental geometry. The counter-propagating detection lasers generate UV photons from the desorbed Na atoms, which are sampled by a photomultiplier (PMT). The pulsed laser (532 nm or 1064 nm) desorbs atoms either from the front side of a PDMS-coated prism or from the evanescent wave.

independence of kinetic energies on desorption wavelength [12], which in turn means that the initial excitation is decoupled from the final desorption process.

The problem of light-induced alkali-metal desorption becomes more sophisticated if the alkali metal resides in an inert but complex polymeric mesh—i.e., a three-dimensional, flexible dielectric reservoir. Some time ago [4,13] it has been observed that PDMS (polydimethylsiloxane) thin films on dielectrics fulfill the main conditions for such a reservoir, being an inert environment that can be filled with alkali metals and emptied by shining nonresonant, low-power light on it. The effect has been called LIAD. Applied to glass containers coated with PDMS it results in a reproducible and high-vacuum compatible way of storing and releasing alkali-metal atoms for, e.g., filling magnetooptical traps [14]. Since its first observation, the LIAD effect has been reported also for OCT (octamethylcyclotetrasiloxane) and for paraffine [7]. The repeating unit of PDMS is -Si$(CH_3)_2$-O-, and the typical number of repeat units used in the present experiment is 500.

Since the coils of PDMS are highly flexible [15], it is the most highly compressible among the long-chain polymers. As a result of this flexibility, PDMS is amorphous with a glass transition temperature of 144 K and a melting temperature of 232 K. In all experiments reported here the surfaces have been above those temperatures and thus PDMS has always been in its rubbery state.

In this paper we determine the kinetic energy distributions of Na and rubidium atoms desorbed from PDMS thin films via pulsed laser-induced desorption with the desorption laser hitting the films both via the evanescent wave and via normal incidence illumination. From the kinetic energy distributions we determine barrier heights of the potentials relevant for desorption from PDMS.

II. EXPERIMENT

The experimental setup for Na atom desorption is sketched in Fig. 1. More details are given in [16]. The setup consisted of a PDMS-coated glass prism, which was mounted in a high-vacuum chamber ($p_0 \simeq 10^{-7}$ torr) on a translationally movable, rotatable, and coolable manipulator ($T_i = 260-300$ K). Surface temperatures T_i were measured with a Ni-NiCr thermocouple on the manipulator, which was calibrated with the help of a second thermocouple firmly glued with thermoconducting paste onto the glass surface. Sodium was deposited onto the hypotenuse of the prism by running a current of about 7 A through a Na dispenser (SAES getters). Optical extinction measurements have shown that Na cluster formation on top of or in the PDMS film is negligible under our conditions.

Na atoms were desorbed from the prisms hypotenuse by focusing the beam of a Nd-YAG laser (continuum powerlite 8000, 10 Hz) on it from either the front side or through the prism short side. The latter geometry resulted in an evanescent wave on either the plain prisms hypotenuse or the surface of the PDMS-coated hypotenuse. The penetration depth of the evanescent wave depends on the refractive indices of prism and PDMS and the wavelength of the desorption laser (1064 nm or 532 nm) as well as the angle of incidence onto the hypotenuse. For the present experiments it ranged between 100 nm and 1.5 μm.

A shutter inside the vacuum chamber in front of the entrance window for the desorption laser was closed during sodium atom adsorption in order to keep the window free of sodium atoms. Hence laser-induced desorption of sodium atoms from that window did not congest the measurements. A beam dump was added at the output side of the prism so as to suppress desorption from the chamber walls and exit windows.

For the investigation of Rb atom desorption we have used PDMS-coated glass slides, which were loaded in a separate vacuum chamber with Rb and afterwards transferred in a desorption chamber. For loading at a background pressure of 5×10^{-7} mbar a reservoir with a natural mixture of Rb atoms was heated to about 330 K and the sample was exposed to the Rb vapor for a few hours to days. The background pressure in the desorption chamber was of the order of 10^{-9} mbar. By separating deposition and desorption process

we have avoided problems with a Rb coverage of the walls in the desorption chamber and also were able to mimic the PDMS filling process in a glass cell environment.

Rb atoms were desorbed solely from the front side of the glass slides by illumination with a 7-ns, 5-Hz Nd:YAG laser.

Na atoms were detected after desorption by exciting them with two photons in the focal point of two counterpropagating lasers, tuned onto resonance transitions from the ground state ($3S_{1/2} \rightarrow 3P_{3/2}$) and from the excited state ($3P_{3/2} \rightarrow 5S_{1/2}$) (TPLIF, two-photon laser-induced fluorescence). The lasers were a tunable single-mode ring dye laser at frequencies around 16 973.35 cm^{-1} ($3S_{1/2} \rightarrow 3P_{3/2}$) and a tunable linear dye laser at frequencies around 16 227.31 cm^{-1} ($3P_{3/2} \rightarrow 5S_{1/2}$), both pumped by an argon-ion laser. Following the resonant two-photon transition the 330-nm photons from the $4P \rightarrow 3S$ transition were collected by a photomultiplier behind an interference filter ($\Delta\lambda = 10$ nm).

For detection of the desorbed Rb atoms we have used diode-laser-induced one-photon fluorescence following light absorption via the 794.5 nm Rb D_1 line. Two interference filters were placed in front of the photomultiplier in order to decrease the background signal intensity.

Time-of-flight (TOF) measurements were performed using a multichannel analyzer with box sizes from 10 to 80 ns, which was triggered by the desorption laser pulse (8 ns duration) and the arrival time of the desorbed atoms within the focus of the two continuous-wave detection lasers. Typical distances between desorption laser spot on the hypotenuse (a few millimeters diameter) and detection focal point (0.5 mm diameter) were $\Delta x = 9-40$ mm. The temporal resolution for thermal atoms was of the order of 1 μs due to the finite detection lasers diameter.

Two background contributions had to be taken care of while analyzing the TOF data. First, the desorption-laser (532 nm) induced luminescence in the PDMS film at fluences higher than 330 mJ/cm^2 and it showed incubation behavior; i.e., the signal intensity changed with number of irradiating pulses due to a photophysical and photochemical modification of the PDMS film [17]. For 1064 nm light desorption this effect was not visible since the PDMS is essentially transparent for these low-energy photons [16,18]. In addition, scattered photons from the desorption laser were detected by the photomultiplier, which has been taken into account as a single decay curve for finally fitting the TOF distributions.

III. RESULTS

Figure 2 shows a TOF measurement for desorption of sodium together with a fit curve being the sum of two theoretical plots—namely, the signal from the atoms desorbed from the prism, assuming a Maxwell-Boltzmann distribution,

$$I(t) \propto t^{-4} \exp\left[-\frac{m\Delta x^2}{2t^2 k_B T} \right] \tag{1}$$

and a second signal due to scattered photons.

In Eq. (1), m is the mass of the alkali-metal atoms, Δx the TOF distance, k_B Boltzmann's constant, t the time, and T the temperature of the flux-corrected Maxwellian distribution. In the following we will characterize the observed signals in terms of T, remembering that the most probable kinetic energy of the desorbed atoms is given by $E_{mp} = k_B T$.

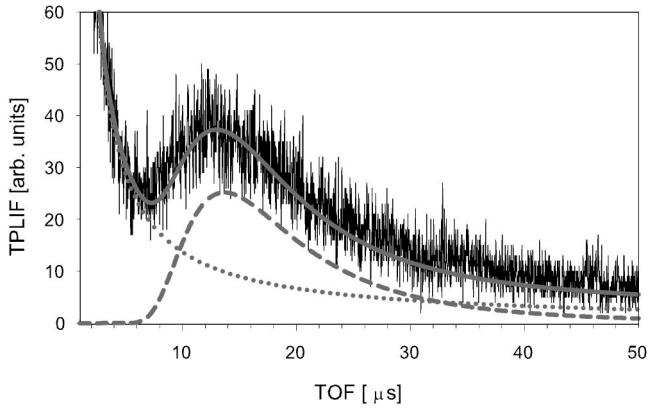

FIG. 2. Typical evanescent-wave desorption spectrum (532 nm) for Na desorption from PDMS at $\Theta_i = 48°$. $F_L = 180$ mJ/cm^2, $\Delta x = 28$ mm, and $T_i = 295$ K. The dashed line is the Maxwellian TOF distribution, the dotted line is a background contribution, and the solid line is the sum of the dashed and dotted line. $T = 3000$ K.

The data collected in Fig. 2 have been taken with the desorption laser incident at $\Theta_i = 48°$ and those in Fig. 3 under front-side irradiation. TOF measurements were performed with different desorption laser intensities (90–311 mJ/cm^2 for 1064 nm light and 50–300 mJ/cm^2 for 532 nm light) from the front side and at two different angles of incidence (48° and 66°) in the evanescent-wave configuration. A plot of temperatures versus F_L (Fig. 4) for Na shows a linear dependence of the kinetic energies of the desorbed atoms on F_L, not depending on the angle of incidence. The fluence has been corrected for the change in area in the prism hypotenuse resulting from different angles of incidence. However, it has

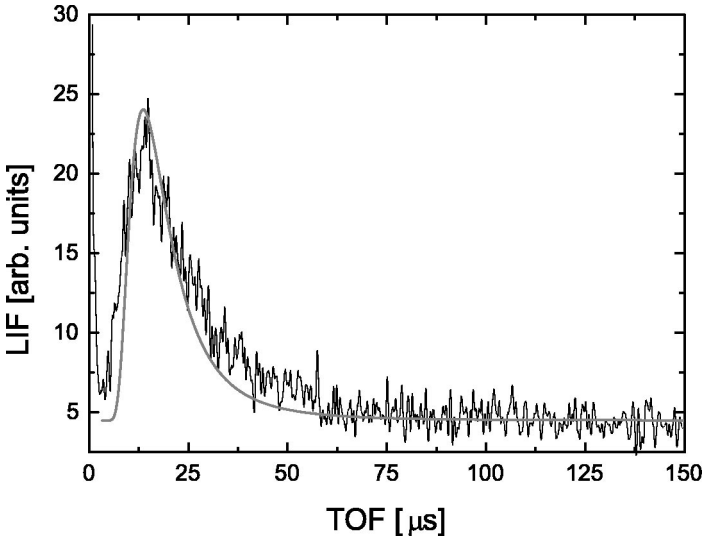

FIG. 3. TOF spectrum obtained following 1064 nm desorption of Rb from PDMS using normal incidence irradiation. $F_L = 311$ mJ/cm^2, $\Delta x = 9$ mm, and $T_i = 295$ K. The smooth line is a Maxwellian TOF distribution.

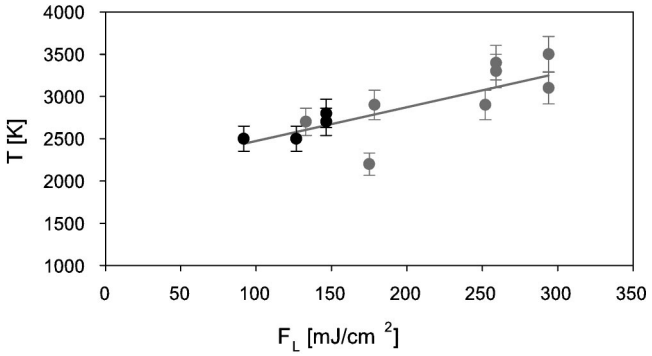

FIG. 4. Evanescent wave-desorption (1064 nm) of Na from PDMS. Gray data: $\Theta_i = 48°$ Black data: $\Theta_i = 66°$. $T_i = 260$ K. The line is a linear regression to the data.

not been corrected for possible changes due to the dependence of the intensity of the evanescent wave on the angle of incidence.

Figure 5 shows a plot of the velocity-corrected maximum desorption rate Y_{max} as a function of F_L for desorption in the evanescent wave. The data are based on measurements made by depositing sodium for 5 min each on the cooled sample before performing the next desorption measurement.

The measured temperatures as a function of F_L both for *s*- and *p*-polarized 532 nm light are shown in Fig. 6. As in the case of the 1064 nm desorption light there is a linear dependence between T and F_L. This dependence was not influenced by the time interval between the measurements. Hence it is not due to chemical changes in the PDMS following irradiation with the desorption laser.

Note that the fluences of the desorption laser in Fig. 6 have not been corrected for the dependence of the intensity of the evanescent wave on the polarization. Since T depends on F_L and since the intensity of *p*-polarized light on the surface is about a factor of 2 larger than that of *s*-polarized light, one would expect to see different curves $T(F_L)$ for *p*- and *s*-polarized desorption. This is obviously not the case.

TOF measurements made using front-side excitation showed the same dependence of T on F_L.

Figure 3 shows for comparison the best Maxwellian fit for a TOF spectrum obtained for desorbed Rb atoms. A significant disagreement between measurement and fitting is observed, indicating that the desorbing flux does not follow a

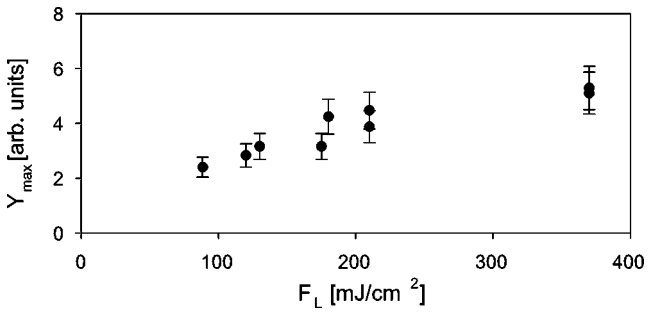

FIG. 5. Maximum desorption rate for evanescent-wave desorption (1064 nm) of Na from PDMS. $\Theta_i = 48°$, $T_i = 260$ K, and $\Delta x = 30$ mm.

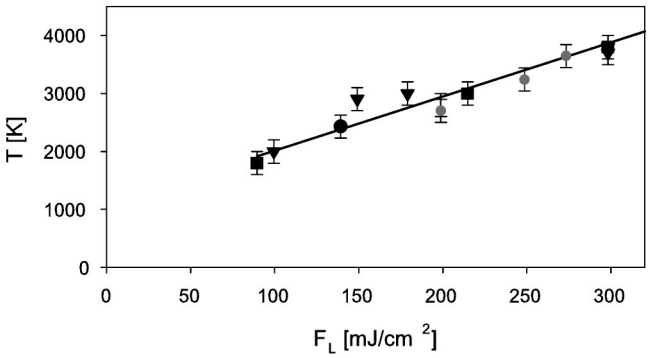

FIG. 6. Evanescent-wave desorption (532 nm) of Na from PDMS. $\Theta_i = 48°$ and $T_i = 260$ K. Gray data: *p*-polarized light. Black data: *s*-polarized light. The different symbols are for measurements done on different days.

Maxwellian distribution. Figure 7 shows a plot of the most probable kinetic energies of the desorbed Rb atoms, determined from the maxima of the time-of-flight distributions, as a function of fluence. We find an average value of $E_{mp} = 200 \pm 70$ meV or an equivalent temperature of $T = 2300 \pm 800$ K, which does not depend on the fluence.

IV. DISCUSSION AND CONCLUSIONS

The kinetic energies of the desorbed Na atoms were found to depend on the desorption laser fluence both with desorption by 1064 nm and 532 nm light. No dependence of the kinetic energies on the polarization or on the angle of incidence was found, other than that from the change in area of the desorption laser. Hence the laser interaction (heating) occurs not in the evanescent-wave regime but in the bulk of the film. Note that the largest TPLIF intensities were obtained by depositing sodium on a cooled sample and then allowing it to warm up. Longer deposition times did not result in larger TPLIF intensities but allowed more measurements to be made before the film was depleted of sodium. For Rb desorp-

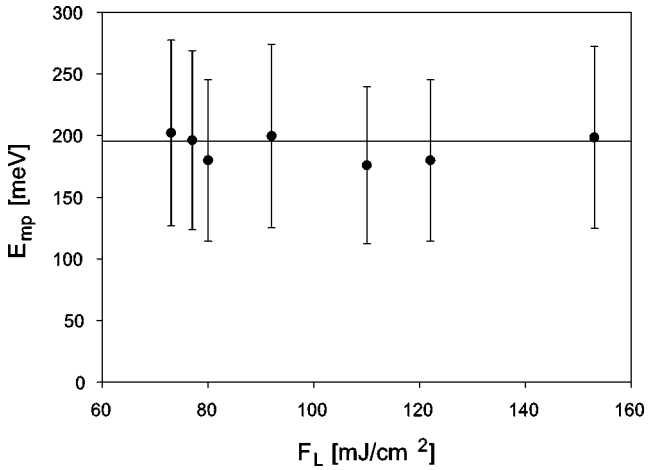

FIG. 7. The most probable kinetic energy of Rb atoms desorbed from PDMS using normal incidence irradiation (1064 nm). $T_i = 295$ K. The line is a linear regression to the data.

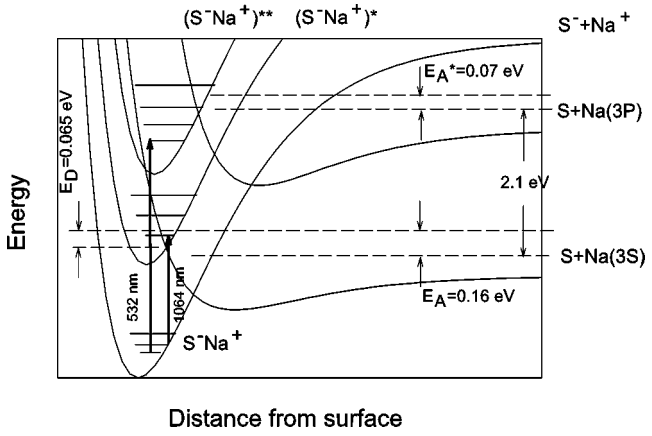

FIG. 8. Proposed scheme of terms explaining the photodesorption process. The excitation of the charge transfer complex being in the ground electronic state state S^-Na^+ either by 1064 nm or 532 nm light leads to a transition to the excited state $(S^-Na^+)^*$ or $(S^-Na^+)^{**}$, respectively. A fast thermalization results in a Boltzmann distribution over the vibrational levels within each term. The subsequent desorption runs from the vibrational levels which are above the potential barriers E_A or E_A^*, depending on which term was initially excited.

tion the signal decreased during illumination, but turning off the illumination resulted in an afterwards increased intensity. This points towards a desorption process influenced by diffusion of atoms in the bulk of the PDMS film.

Extrapolating the kinetic energies of the desorbed atoms as a function of the desorption laser fluence to low fluences we find markedly different values for different photon energies. These values are determined by the potential barriers below which atoms cannot be desorbed. This means that desorption runs along different pathways when induced by 1064 nm vs 532 nm light. However, in both cases the most probable kinetic energy of the desorbed atoms is linearly increasing with laser fluence, suggesting that desorption starts from thermally equilibrated states and that the corresponding temperature is proportional to the laser fluence.

The energy diagram shown in Fig. 8 describes that behavior semiquantitatively. We assume that the ground state of the adsorbed species is the charge transfer complex S^-Na^+, where S denotes the PDMS substrate [19]. This complex can have two or more excited electronic states $(S^-Na^+)^*$ and $(S^-Na^+)^{**}$. Besides that, there are two electronic states corresponding to physical adsorption of a neutral Na atom in the ground state $3S$ and in the excited state $3P$. The illumination of the adsorbate complex by 1064 nm and 532 nm light leads to the excitation of different electronic states. It is reasonable to assume that a wavelength of 1064 nm falls in the absorption band for the transition $S^-Na^+ \rightarrow (S^-Na^+)^*$ whereas a wavelength of 532 nm corresponds to the absorption band $S^-Na^+ \rightarrow (S^-Na^+)^{**}$. The electronic excitation is followed by a fast vibrational relaxation due to the coupling of the complex vibrations to the phonon bath of the PDMS film. The typical time of such thermalization (subpicoseconds) is much shorter than both the relaxation time to the ground electronic state and the adsorption time. This means that the equilibrium (Boltzmann) populations of the vibrational levels in the excited electronic term are established prior to desorption. Hence desorption occurs in thermal equilibrium with respect to the nuclear subsystem.

The potential barriers originating from the crossings of the electronic terms $(S^-Na^+)^*$ and $S+Na(3S)$ as well as $(S^-Na^+)^{**}$ and $S+Na(3P)$ determine the desorption dynamics. If the charge transfer complex lies energetically on vibrational levels above the crossing points, this might result in ground-state or electronically excited neutral sodium atoms, respectively, having the same total energy.

The probability for such a process can be calculated using the Landau-Zener formula provided that the parameters of both terms are known [20]. The most probable kinetic energy of desorbed atoms is then determined as $E_{mp}=E_A+k_BT_s$ with E_A the height of the barrier with respect to the energy of an atom far from the surface and T_s the surface temperature. For small laser fluences the surface temperature remains on its initial value T_i and hence the value of E_{mp} obtained by linear extrapolation of the measured dependence to $F_L=0$ equals $E_A+k_BT_i$. This finding allows one to deduce from the measured values $E_A=(160\pm30)$ meV for desorption of Na in the state $3S$ and $E_A^*=(70\pm20)$ meV for desorption in the state $3P$.

It should be noted that in the picture suggested above the desorption is induced by wavelengths which are within the absorption bands corresponding to the transitions $S^-Na^+ \rightarrow (S^-Na^+)^*$, $(S^-Na^+)^{**}$. In Ref. [19] the frequency threshold for desorption of Na atoms from PDMS was found to be 9500 cm^{-1}. The wavelength 1064 nm corresponds to 9398 cm^{-1}— i.e., 102 cm^{-1} below this threshold. The latter quantity has a magnitude typical for vibrational excitations. This finding means either that the absorption leading to desorption starts from an excited vibrational level or that PDMS phonons participate in this process.

Note that the temperature which characterizes the desorption process is high although the PDMS film is transparent in the spectral range under consideration. This might be explained by "resonant heating," suggested for the photodesorption of molecules by resonant infrared radiation [21], where resonant laser-molecular vibrational coupling can lead to a strong surface heating through transfer of the laser energy that has been absorbed in the internal vibration of the adsorbed molecule into substrate phonons. In the case of the present electronic excitation, the energy level in the excited electronic term is degenerate with an excited vibrational level of the ground-state electronic term. If the two terms cross each other, the transfer from the excited- to the ground-state term can be very efficient when passing above the crossing point in the course of vibrational motion [22]. In that case the charge transfer complex appears in a highly excited vibrational state. In turn, the vibrational excitation can be effectively removed by means of generation of the film phonons—i.e., heating of the film.

The increase in surface temperature can be estimated from the following simple model. The sodium atoms distributed in the PDMS film resonantly absorb laser radiation, resulting in a heating of the film. The corresponding temperature field $T(z,t)$ obeys the heat conduction equation

$$\frac{\partial^2 T}{\partial z^2} + \frac{g(z,t)}{k} = \frac{1}{\chi}\frac{\partial T}{\partial t}, \tag{2}$$

where k is the thermal conductivity, χ is the thermal diffusivity, and g is the volumetric heat generation rate. We assume that the latter quantity can be approximated by

$$g(z,t) = \begin{cases} E\delta(t), & -\Delta z \leqslant z \leqslant 0, \\ 0, & z \leqslant -\Delta z, \end{cases} \tag{3}$$

with E the total energy input per unit volume for a pulse and Δz the mean depth of sodium penetration into the film. In such a case Eq. (2) has the solution

$$\Delta T(z,t) = T(z,t) - T_i = \frac{\chi E}{2k}\left[\mathrm{erf}\left(\frac{z+\Delta z}{\sqrt{4\chi t}}\right) - \mathrm{erf}\left(\frac{z-\Delta z}{\sqrt{4\chi t}}\right)\right], \tag{4}$$

where erf(x) is the error function. Now the surface temperature increase ΔT_s which is relevant to the desorption process is obtained as

$$\Delta T_s(t) = \Delta T(0,t) = \frac{\chi E}{k}\mathrm{erf}\left(\frac{\Delta z}{\sqrt{4\chi t}}\right). \tag{5}$$

Its maximum value

$$\Delta T_{sm} = \frac{\chi E}{k} \tag{6}$$

is reached during the pulse at $t=0$. The δ function in Eq. (3) implies that the laser pulse duration is much shorter than the characteristic time of the problem, $\tau=(\Delta z)^2/4\chi$. Taking $\Delta z \sim 1\ \mu$m and $\chi \sim 10^{-3}$ cm^2/s we obtain $\tau \sim 2.5\ \mu$s—i.e., much longer than the duration of the desorption laser pulse of 8 ns. That confirms the validity of this approximation.

The quantity E can be estimated as follows. The energy absorbed in a unit volume during the pulse can be found as $E_{ab}=\alpha F_L$ with α the absorption coefficient of sodium atoms distributed in the film. We assume that the energy of the electronic state excited by light can be transferred into the film phonon modes with probability p. Then we come to the relation $E=p\alpha F_L$. Its substitution into Eq. (7) gives a linear dependence of the surface temperature on the laser fluence. Since we do not have data for α, we derive conclusions from previous measurements on the LIAD effect for sodium atoms. For that we note that $\alpha=\sigma N$ with σ the absorption cross section for a sodium atom in the film and N the volume number density of sodium atoms. It was reported [19] that the increase in the gas-phase Na atom density following irradiation of a Na-filled and PDMS-coated cell is typically five orders of magnitude greater than the normal room-temperature vapor pressure of the Na metal. Taking the latter quantity to be 10^{-8} Pa, we obtain for the LIAD effect a pressure of sodium atoms of 10^{-3} Pa. This pressure corresponds at room temperature to an atom number density of 2.3×10^{11} cm^{-3}. Assuming that the linear dimensions of the gas cell are of the order of a few cm, we conclude that the total amount of sodium atoms contained in the PDMS film per cm^2 is about 10^{12}. Taking the thickness of the film to be of the order of 1 μm we estimate $N \sim 10^{16}$ cm^{-3}.

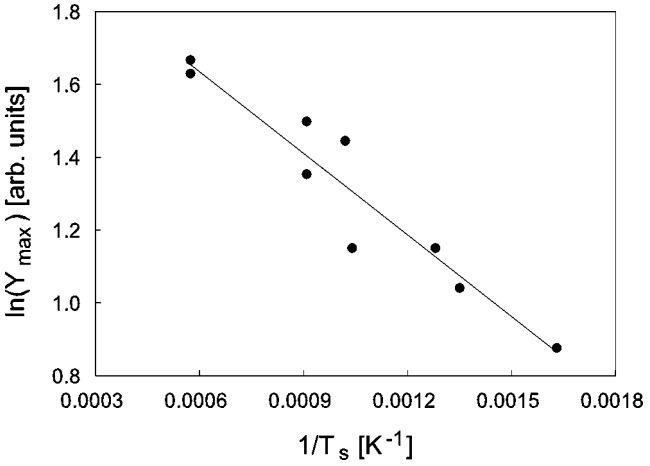

FIG. 9. Logarithm of the photodesorption yield plotted vs the inverse surface temperature determined from the linear fit of the dependence T vs laser fluence. Its slope gives the value of the potential barrier for desorption.

The quantities p and σ are unknown and we have to estimate them also. We believe that the absorption cross section should be comparable with the value of 3×10^{-16} cm^2 obtained for Na atoms adsorbed on sapphire which is transparent in the visible range [23]. For effective Landau-Zener transitions one can take $p \sim 1$. The thermal parameters of PDMS are $\chi=1.08\times10^{-3}$ cm^2/s [24] and $k=1.7 \times 10^{-3}$ W/cm K [25]. As a result we obtain, for the slope of the dependence T versus F_L, $\Delta T_{sm}/F_L \sim 2$ cm^2 K/mJ. This value is of the same order of magnitude as the slopes determined from the measured dependences of 4.0 cm^2 K/mJ for 1064 nm and of 9.3 cm^2 K/mJ for 532 nm.

Once we know the relation between the laser fluence and the surface temperature given by the linear fits in Figs. 4 and 6, we can deduce some additional information on the desorption dynamics from the dependence of the desorption rate versus the laser fluence (Fig. 5). Assuming that the surface number density of sodium atoms does not change strongly during the laser pulse, we expect that the desorption yield Y is proportional to the desorption rate

$$w(T_s) = \nu \exp\left(-\frac{E_D}{k_B T_s}\right), \tag{7}$$

where ν is the frequency of vibrations in the state from which the desorption occurs and E_D is the potential barrier for desorption counted from the potential well bottom. Recalculating the surface temperature from the linear fit given in Fig. 5, we plot in Fig. 9 the logarithm of the desorption yield versus T_s^{-1}. From the linear fit of this dependence we obtain $E_D=(65\pm8)$ meV. Taking $T_i=260$ K and as an estimate $\nu=10^{12}$ s^{-1}, we get for the time of adsorption in the state $(S^-Na^+)^*$ $\tau_a=w^{-1}=18$ ps. This verifies the assumption about thermally equilibrium desorption from this state.

The small value for E_D is consistent with the fact that there is a frequency threshold of 9500 cm^{-1} (1052 nm) for

the sodium desorption [19]. In fact, if the absorption band $(S^-Na^+) \rightarrow (S^-Na^+)^*$ begins from the wavelengths 1064–1052 nm, then in this range an effective desorption over the barrier can be induced even at room temperature with weak light intensities, which is a characteristic of the LIAD effect.

In the case of Rb desorption a qualitatively different situation is observed. We assume that for Rb atoms in the PDMS film a system of terms similar to the one shown in Fig. 8 is relevant, but with different parameters. From the results shown in Fig. 3 and 7, we conclude that 1064 nm light leads to excitation of the charge transfer complex S^-Rb^+ to a vibrational level of the term $(S^-Rb^+)^*$ wxchich lies above the crossing point of the terms $(S^-Rb^+)^*$ and $S+Rb(3S)$. Then direct desorption by means of the Landau-Zener transition occurs and the characteristic time of this process is determined by the period of vibrations in the $(S^-Rb^+)^*$ term which can be comparable with the time of thermalization. This picture suggests that the equilibrium populations of the vibrational levels had not been established prior to desorption and the desorbing flux is non-Maxwellian. In such a case the quantity E_{mp} is determined by the excess of total energy which the charge transfer complex acquires on excitation above the energy level of the compound $S+Rb(3S)$ when an Rb atom is far from the surface.

In summary, we conclude that the dynamics of photodesorption of alkali-metal atoms from a PDMS substrate is ruled by the relative position of the energy level which is initially populated by photoexcitation. If this level lies below the crossing point between the excited term of the charge transfer complex and the term for physically adsorbed atoms, then desorption occurs after thermalization. The resulting desorption flux is Maxwellian with the temperature determined by "resonant heating." If this level lies above the crossing point, the direct desorption runs from a thermally nonequilibrium state. In such a case the most probable kinetic energy of the desorbed atoms is determined by the light quantum of energy.

ACKNOWLEDGMENTS

J.B. acknowledges the financial support provided through the European Community's Human Potential Programme under Contract No. HPRN-CT-2002-00304, FASTNet. We are grateful to the Danish Research Agency SNF and to NATO via CLG Grant No. 979024 for further support. We thank K. Rubahn for sample preparation and J.R. Manson and V.V. Petrunin for stimulating discussions.

[1] J. R. Manson, M. Renger, and H.-G. Rubahn, Phys. Lett. A **224**, 121 (1996).
[2] B. V. Yakshinskiy and T. E. Madey, Surf. Sci. **451**, 160 (2000).
[3] B. V. Yakshinskiy and T. E. Madey, Surf. Sci. **528**, 54 (2003).
[4] A. Gozzini, F. Mango, J. H. Xu, G. Alzetta, F. Maccarrone, and R. A. Bernheim, Nuovo Cimento D **15**, 709 (1993).
[5] S. N. Atutov *et al.*, Phys. Rev. A **60**, 4693 (1999).
[6] C. Marinelli, K. A. Nasyrov, S. Bocci, B. Pieragnoli, A. Burchianti, V. Biancalana, E. Mariotti, S. N. Atutov, and L. Moi, Eur. Phys. J. D **13**, 231 (2001).
[7] E. B. Alexandrov *et al.*, Phys. Rev. A **66**, 042903 (2002).
[8] D. V. Chakarov, L. Österlund, B. Hellsing, V. P. Zhdanov, and B. Kasemo, Surf. Sci. Lett. **311**, L724 (1994).
[9] M. Wilde, I. Beauport, F. Stuhl, K. Al-Shamery, and H.-J. Freund, Phys. Rev. B **59**, 13 401 (1999).
[10] A. M. Bonch-Bruevich, Yu. N. Maksimov, S. G. Przhibels'kii, and V. V. Khromov, Sov. Phys. JETP **65**, 161 (1987).
[11] W. Hoheisel, M. Vollmer, and F. Traeger, Phys. Rev. B **48**, 17 463 (1993).
[12] F. Balzer, R. Gerlach, J. R. Manson, and H.-G. Rubahn, J. Chem. Phys. **106**, 7995 (1997).
[13] M. Meucci, E. Mariotti, P. Bicchi, C. Marinelli, and L. Moi, Europhys. Lett. **25**, 639 (1994).
[14] S. N. Atutov *et al.*, Eur. Phys. J. D **13**, 71 (2001).
[15] S. W. Sides, J. Curro, G. S. Grest, M. J. Stevens, T. Soddemann, A. Habenschuss, and J. D. Londono, Macromolecules **35**, 6455 (2002).
[16] J. Brewer, masters thesis, South Danish University, 2003.
[17] V.-M-Graubner, R. Jordan, O. Nuyken, T. Lippert, M. Hauer, B. Schnyder, and A. Wokaun, Appl. Surf. Sci. **197**, 786 (2002).
[18] M. J. Hunter and N. Wright, J. Am. Chem. Soc. **69**, 803 (1947).
[19] J. H. Xu, A. Gozzini, F. Mango, G. Alzetta, and R. A. Bernheim, Phys. Rev. A **54**, 3146 (1996).
[20] L. D. Landau and E. M. Lifshitz, *Quantum Mechanics: Nonrelativistic Theory* (Pergamon Press, New York, 1988), p. 350.
[21] Z. W. Gortel, H. J. Kreuzer, P. Piercy, and R. Teshima, Phys. Rev. B **28**, 2119 (1983).
[22] Note that this process can take place for sodium atoms in the film interior. In that case the term scheme shown in Fig. 8 has to be modified.
[23] A. M. Bonch-Bruevich, Yu. N. Maksimov, and V. V. Khromov, Opt. Spectrosc. **58**, 854 (1985).
[24] A. W. Broerman, D. C. Venerus, and J. D. Schieber, J. Chem. Phys. **111**, 6965 (1999).
[25] Y. S. Shin, K. Cho, S. H. Lim, S. Chung, S.-J. Park, C. Chung, D.-C. Han, and J. K. Chang, J. Micromech. Microeng. **13**, 768 (2003).